Published in final edited form as:
J Occup Environ Hyg. 2017 December ; 14(12): 995–1002. doi:10.1080/15459624.2017.1351614.

Evaluation of a passive method for determining particle penetration through protective clothing materials

Peter A. Jaques[a], **Lee Portnoff**[b]

[a]AECOM, Aiken, South Carolina

[b]National Institute for Occupational Safety and Health (NIOSH), National Personal Protective Technology Laboratory, Pittsburgh, Pennsylvania

Abstract

The risk of workers'exposure to aerosolized particles has increased with the upsurge in the production of engineered nanomaterials. Currently, a whole-body standard test method for measuring particle penetration through protective clothing ensembles is not available. Those available for respirators neglect the most common challenges to ensembles, because they use active vacuum-based filtration, designed to simulate breathing, rather than the positive forces of wind experienced by workers. Thus, a passive method that measures wind-driven particle penetration through ensemble fabric has been developed and evaluated. The apparatus includes a multidomain magnetic passive aerosol sampler housed in a shrouded penetration cell. Performance evaluation was conducted in a recirculation aerosol wind tunnel using paramagnetic $Fe^{3}O^{4}$ (i.e., iron (II, III) oxide) particles for the challenge aerosol. The particles were collected on a PVC substrate and quantified using a computer-controlled scanning electron microscope. Particle penetration levels were determined by taking the ratio of the particle number collected on the substrate with a fabric (sample) to that without a fabric (control). Results for each fabric obtained by this passive method were compared to previous results from an automated vacuum-based active fractional efficiency tester (TSI 3160), which used sodium chloride particles as the challenge aerosol. Four nonwoven fabrics with a range of thicknesses, porosities, and air permeabilities were evaluated. Smoke tests and flow modeling showed the passive sampler shroud provided smooth (non-turbulent) air flow along the exterior of the sampler, such that disturbance of flow stream lines and distortion of the particle size distribution were reduced. Differences between the active and passive approaches were as high as 5.5-fold for the fabric with the lowest air permeability (0.00067 m/sec-Pa), suggesting the active method overestimated penetration in dense fabrics because the active method draws air at a constant flow rate regardless of the resistance of the test fabric. The passive method indicated greater sensitivity since penetration decreased in response to the increase in permeability.

CONTACT Lee Portnoff, LPortnoff@cdc.gov, National Institute for Occupational Safety and Health (NIOSH), National Personal Protective Technology Laboratory, 626 Cochrans Mill Road, Pittsburgh, PA 15236.

Disclaimer
The findings and conclusions in this article are those of the authors and do not necessarily represent the views of the National Institute for Occupational Safety and Health. Mention of any company or product does not constitute endorsement by NIOSH. The authors identify no conflicts of interest in the conduct of this study.

Keywords

Aerosol; penetration; protective fabric; sampler; test method

Introduction

Protective ensembles are essential for protecting workers against dermal exposure to aerosols that contain potentially toxic particles. Currently, a standardized methodology that examines the barrier effectiveness of a full protective clothing ensemble to particulate hazards does not exist. Previous studies on particle penetration through protective clothing materials have most commonly been conducted with a standardized respiratory filter tester that does not reflect ensemble usage conditions,[1,2] such as the TSI model 8130[3] and, more recently, the TSI model 3160.[4] However, in the workplace, especially in the outdoor environment, penetration is primarily driven by wind and body movement.[5-8] In addition, the wearer behind the protective clothing acts as a blunt body, causing a change in airflow streamlines[8,9] and, thus, the approaching particle trajectories[5,8,10] would behave according to the streamlines, affecting particle penetration through the ensemble. To address this, Hill and colleagues[10] designed a system to measure the barrier protection of woven garments worn by naval workers against particles driven by ambient wind conditions. They tested the penetration of particles between about 2 μm and 20 nm delivered from 9–37 m/sec to a fabric draped around a vertical tube with dimensions similar to a human arm. The system supported the test fabric with a screen and provided an annular region that approximated the air space that exists between loosely fit PPE and the skin. Using measurements at a single point normal to the incoming wind direction, the authors reported a maximum particle penetration size of about 1 μm with the penetration ratio increasing at higher ambient wind speeds. However, results may differ for indoor air exposures where wind speeds are much lower. In a survey of indoor workplaces, Baldwin and Maynard[11] reported that 85% of 55 occupational environments had much lower background wind speeds (less than 0.3 m/sec). Their results include testing an entire suit system for leakage through seams, closures, areas of transition to other protective equipment, and from movement and activities. A system-level aerosol test (i.e., aerosol man-insimulant test [MIST]), similar to the chemical MIST[12] is currently non-existent. Such a test would require 30 passive aerosol dosimeters (approximately 25 × 35 × 2 mm) placed at different locations throughout and under the protective clothing layer worn by a human subject.

Thus, a multidomain magnetic passive aerosol sampler (MPAS) was designed to enable an aerosol MIST.[13,14] The MPAS generates a magnetic force to collect paramagnetic iron (II, III) oxide (Fe^3O^4) particles as the challenge aerosol. The magnetic force of the MPAS provides a much higher collection efficiency than a conventional passive sampler, which allows collecting a sufficient quantity of particles within the time frame of a MIST procedure.[13] The multidomain arrangement allows magnetic force to dissipate within a small distance between the sampler opening and the substrate to avoid overestimating penetration levels caused by pulling particles from the outside of ensembles, and significantly improves the uniformity of magnetite aerosol particle deposition across the substrate. Particle deposition across the substrate was shown to have a consistent pattern which enables measuring reproducible particle numbers using a randomized counting method.[14] The objectives of this study were to develop a benchtop particle penetration cell (i.e., MPAS holder and shroud), to calculate penetration ratios (active/passive), and to correlate penetration ratios with physical characteristics of four fabrics (Table 1). Fabrics in this study were selected by structural feature and are not necessarily typical of protective clothing.

Experimental methods

Design of penetration cell to evaluate passive sampler

A shrouded aluminum penetration cell (SP-Cell) (Figure 1) was designed to simulate conditions of the MPAS for its application in a full-body-ensemble aerosol MIST, where it would be secured to a human body under a test garment. For this, the SP-Cell was structured with the MPAS holder (28 mm) secured to its base 2 mm downstream from the fabric (Figure 2). The MPAS was positioned 2 mm away from the inner surface of the swatch to mimic a typical gap between clothing and the human body.[15] The overall dimension of the SP-Cell (145 mm long) was designed for air flow and particle trajectory passage, through and around the MPAS, to prevent re-entrainment of particles that can be caused by turbulence, significant alteration of flow stream lines, and distortion of the particle size distribution. Since the MPAS was expected to behave like a blunt body when secured to the human body in the MIST, a 6-mm diameter annular space was incorporated between the exterior of the MPAS holder and the inner walls of the SP-Cell holder (cap, base, and shroud) to provide minimum air flow resistance between the fabric swatch and the units' exhaust (d = 10 mm). Also, following the fabric and MPAS housing, the shroud unit had a relatively subtle taper, with the exterior diameter reduced from 51 mm to 12 mm and interior diameter from 40 mm to 10 mm.

The MPAS base is secured by the MPAS holder to the shaft holder, which is threaded to adjust the spacing between the fabric and MPAS particle collection surface; it has a cap to secure the test fabric swatch, and a shaft holder for positioning the SP-Cell onto a multi-cell sampling ring. The shroud section consists of a tapered shroud, which is threaded onto the multi-cell shaft holder, and has a flow control valve at its exhaust end to control the effective flow of air (caused by the ambient wind) that passes through the fabric. A butterfly valve was incorporated to equalize the effective face velocity (V_f) of the control (no fabric) to that of the sample (with fabric).

Four nonwoven fabrics were selected for this study, which included three types of cleaning cloths (Fabrics I, II, and III) and a fabric for making air permeable personal protective garments (Fabric IV) (Table 1). These fabrics consisted of a relatively broad range of physical properties (Table 2). Performance evaluation was conducted in a recirculation aerosol wind tunnel (RAWT)[16] using paramagnetic Fe^3O^4 (i.e., iron (II, III) oxide) particles for the challenge aerosol.[13]

Investigation of flow field

To investigate the ability of the shrouded exhaust unit to minimize possible eddy effects downstream of the sampler, smoke tests were conducted inside the RAWT by comparing downstream air flow between the sampler with and without the shrouded exhaust unit. In addition, the flow field inside and around the SP-Cell was numerically simulated using Computational Fluid Dynamics (CFD) k-ε turbulence model (ANSYS CFX ver. 12.1, Canonsburg, PA).

Performance evaluation of the passive method

For each garment model tested, eight SP-Cells were circumferentially arranged around a cylindrical stand that was attached to the inner surface of the exterior wall of the RAWT with four co-located pairs of samples (with swatch) and controls (without swatch) (Figure 3). Percent particle penetration was calculated using a configuration having four samples and four controls by Equation (1)

Percent particle penetration (PPP):

$$PPP = avg.\ (S_1 + S_2 + S_3 + S_4)\ /\ avg. \times (C_{snf1} + C_{snf2} + C_{snf3} + C_{snf4}), \quad (1)$$

where S is the particle count with fabric sample and C_{snf} is the particle count without fabric sample.

Previously, the air velocity was shown to be concentrically uniform at each sector, but with a gradual decrease in uniform flow approaching the wind tunnel walls.[16] Thus, the position of the samples and controls were alternated to minimize potential variations in particle trajectories between locations. Penetration testing was conducted for 20 minutes at wind speeds ranging from 1.5–3.0 m/s. Polydisperse Fe^3O^4 powder (Alfa Aesar 12962, Puratronic, 99.997%, Ward Hill, MA) was generated and delivered as an aerosol via a Six-Jet Atomizer (Model 9306, TSI Incorporated, Shoreview, MN). The particle concentration inside the RAWT was measured to be approximately 20,000 particles/cm^3 using a scanning mobility particle sizer (SMPS; model 3936, TSI, Incorporated, Shoreview, MN). Particles were collected by the MPAS with a 25 mm Isopore™ polycarbonate substrate, and quantitatively analyzed using computer controlled scanning electron microscopy (CCSEM).[14]

Three sets of challenges for each fabric model were conducted, and three effective face velocities (V_f) (0.25, 0.375, and 0.5 cm/sec) were setup by adjusting the butterfly valve to a predetermined flow according to the swatch diameter. For each delivered wind speed, the effective face velocity was about 20% of the delivered wind speed, depending on the resistance of the fabric. Exhaust flow was measured with a mass flow meter (TSI, model 3063) connected by a 22.9 cm tube that extended outside the RAWT to prevent the meter from affecting flow.

Results and discussion

Airflow differences without (Figure 4a) and with (Figure 4b) the shrouded unit show that no significant air recirculation was present at the exhaust region of the SP-Cell. Downstream turbulence was observed without the shroud; while a smoother smoke plume was observed with the shroud.

Numerical simulation showed that the screen of the SP-Cell created a pressure differential that oriented velocity vectors more directly toward the MPAS (Figure 5). As airflow approached the SP-Cell, velocity decreased and vectors upstream diverged. Airflow was generally smooth near the screen and symmetrical around the SP-Cell for a majority of air flows around the SP-Cell. Inside the SP-Cell, velocity vectors were oriented toward the outlet on the downstream side of the MPAS, and air velocity was about 500-fold lower than wind speed. From this, it was assumed that the SP-Cell with the shrouded exhaust unit would be able to prevent particle re-entrance to the MPAS after exiting the exhaust outlet.

The effective face velocity (V_f) driven by ambient wind speed showed an increase in pressure drop with V_f and substantially different pressure drops across each fabric and between fabric model (Figure 6).

Particle penetration through a representative fabric model (I) using the SP-Cell at the minimum and maximum tested face velocities is shown (Figure 7a). This figure does not indicate a “Most Penetrating Particle Size” (MPPS). The fractional penetration value (S/C) is computed by dividing the sample (S) penetration by control (C) penetration values for each particle size. Comparison between the passive (SP-Cell) and active sampling shows that penetration increases with increasing face velocity for both methods, and penetration for the active method is substantially greater for all conditions (Figure 7b). The active to passive ratio (A/P) varied between 1.5 and 5.5 and generally decreased with an overall increase in penetration, suggesting that it likely overestimated particle penetration by forcing particles through that which would have passed by naturally.

The difference between methods may be partially explained by differences in penetration as a function of the fabric’s physical parameters (Figure 8). Although the results are not direct comparison of each parameter (i.e., all four qualities change in each fabric) it appears that particle penetration through the SP-Cell (passive method) increased with larger fiber diameter (all fabrics), pore area (except for Fabric IV), and air permeability (except for Fabric IV), but decreased with fabric thickness (except for Fabric III). Most of these results are expected. For example, it is expected that the greater surface area provided by smaller fibers, and the flow restriction by smaller pores would reduce particle penetration. Additionally, it would be expected that penetration would increase with a higher air permeability, since permeability is positively associated with increases in air velocity and air pressure. The results of Fabric IV having the lowest penetration, but highest air permeation, may be explained in that it is the thickest, has the smallest fiber diameter, and the second smallest pore area, providing a long tortuous path for particles to pass. The fabric is used as insulation for fire fighter ensembles, and is designed to provide breathability and prevent particle penetration. In contrast Fabric III, which had the second lowest penetration overall, did not have the second lowest penetration as a function of pore size. This is likely because it was a four-layered structure, with the two inner layers reinforced with yarn, providing supplemental protection from particles, and effectively reduced its penetration with respect to pore area.

Although not entirely what we expected, in that a dominant MPPS does not result for all fabrics at all face velocities, these results may reasonably represent penetration that occurs through protective clothing worn by workers. For example, 1–.5 m/sec winds likely predominantly pass around the human body, which acts as a blunt body. A small fraction of air may penetrate through the worn clothing, potentially transporting particles similar to these findings (e.g., for fabrics with similar weave, porosity, and pressure drop).

Summary and conclusion

This study found that particle penetration measured by the SP-Cell (passive method) increased with increasing face velocity, while penetration obtained by the active method was nearly six times greater than that measured by the passive method. Generally, the ratio of active to passive penetration increased with decreasing permeability, and decreased with decreasing pore area for all four fabrics. Since particles are not filtered by worn ensembles as they are for respirators, but can penetrate by wind, these results suggest that the active method overestimated penetration. Fabric IV, used as insulation for fire fighter ensembles, was the thickest fabric with the smallest fiber diameter, which showed a much greater ratio between active and passive methods, likely because of the effects of its greater surface area and lower residence time on particle deposition. Smoke tests in the wind tunnel visually showed that the penetration cell with a shrouded exhaust unit was able to minimize possible eddy effects downstream of the sampler. The results suggest that the shrouded exhaust unit could reduce the potential for particle re-entrainment from the exhaust of the SP-Cell, and thus, avoid overestimations of particle penetration. Limitations of this study include the use of two different lab test aerosols that are not commonly exposed to workers. The quantification of particles by this method was time consuming and a challenge to conduct. Additional work should explore a rapid and easy method for counting particles. A follow-up study would apply the MPAS to an aerosol MIST test by first evaluating its performance of measuring particle penetration through full-ensemble garments worn by a manikin in an aerosol wind tunnel of adequate size. This would be paired with measurements made using an SMPS on the inside and outside of a swatch wrapped around a screened tube housed in various sections of the manikin.[17]

Acknowledgments

The authors acknowledge Mr. Tony Rozzi and Ms. Lisa Barkand formerly with NIOSH for conducting experiments; NIOSH colleagues Teresa Barone, Teh-hsun B. Chen, and Ziqing Zhuang for reviewing this article. Dr. Pengfei Gao served as the project officer during the time this data was collected.

References

[1]. Bergman W, Garr J, and Fearon D: Aerosol penetration measurements through protective clothing in small scale simulation tests. In International Symposium on Protection against Chemical Warfare Agents: Proceedings, G., Gunnar Bloom. Diane Publishing Co., 1989. pp. 61–62.

[2]. US Army: Test operations procedure (TOP) 8-2-501, permeation and penetration of air-permeable, semipermeable, and impermeable materials with chemical agents or simulants (swatch testing). Final report No. AD-A–322329/4/XAB. Dugway Proving Ground, UT (United States). Department of the Army (United States), 1997. p. 79.

[3]. Janssen LL, Bidwell JO, Mullins HE, and Nelson TJ: Efficiency of degraded electret filters: Part I – laboratory testing against NaCl and DOP before and after exposure to workplace aerosols. J. Int. Soc. Respir. Protect 20:71–80 (2003).

[4]. Rengasamy S, Miller A, Eimer BC, and Shaffer RE: Filtration performance of FDA-cleared surgical masks. J. Int. Soc. Respir. Protect (1):54–70 (2009).

[5]. Fedele PD: Model of aerosol protection offered by permeable protective garments. In Performance of Protective Clothing: Fourth Volume, ASTM International, 1992. pp. 3–14.

[6]. Fedele PD, Bergman W, McCallen R, and Sutton S: Hydrodynamically induced aerosol transport through clothing. In The 1986 Army Science Conference. West Point, NY, 1987. pp. 279–293.

[7]. Gao P, Jaques PA, Hsiao T-C, et al. : Evaluation of nano- and submicron particle penetration through ten nonwoven fabrics using a wind-driven approach. J. Occup. Environ. Hyg 8(1):13–22 (2011). [PubMed: 21154104]

[8]. Lei L, Jiangge L, and Daiyun C: Aerodynamic adsorption of permeable chemical protective suit. AIHAJ 62(5):559–562 (2001). [PubMed: 11669381]

[9]. Kim T, and Flynn MR: Airflow pattern around a worker in a uniform freestream. AM. Industr. Hyg. Assoc. J 52(7):287–296 (1991).

[10]. Hill MA, Ghee TA, Kaufman J, and Dhaniyala S: Investigation of aerosol penetration through individual protective equipment in elevated wind conditions. Aer. Sci. Technol 47(7):705–713 (2013).

[11]. Baldwin PE, and Maynard AD: A survey of wind speeds in indoor workplaces. Ann. Occup. Hyg 42(5):303–313 (1998). [PubMed: 9729918]

[12]. ASTM International: Standard Test Method for Man-In-Simulant Test (MIST) for Protective Ensembles (ASTM F2588-2012). [Standard] West Conshohocken, PA: ASTM, 2012.

[13]. Hsiao T-C, Jaques PA, and Gao P: A multidomain magnetic passive aerosol sampler: development and experimental evaluation. Aer. Sci. Technol 47(1):37–45 (2013).

[14]. Jaques PA, Hopke PK, and Gao P: Quantitative analysis of unique deposition pattern of submicron $Fe^{3}O^{4}$ particles using computer-controlled scanning electron microscopy. Aer. Sci. Technol 46(8):905–912 (2012).

[15]. Roberts M, Jamriska M, Skvortsov A, and McCallum R: Study on aerosol penetration through clothing and individual protection equipment. Report No. DSTO-TR-2283. Defense Science and Technology Organization. Australian Dept. of Defense, 2009. p. 32.

[16]. Jaques PA, Hsiao T-C, and Gao P: A recirculation aerosol wind tunnel for evaluating aerosol samplers and measuring particle penetration through protective clothing materials. Ann. Occup. Hyg 55(7):784–796 (2011). [PubMed: 21831849]

[17]. Hill MA, Ghee TA, Kaufman J, and Dhaniyala S: Investigation of aerosol penetration through individual protective equipment in elevated wind conditions. Aer. Sci. Technol 47(7):705–713 (2013).

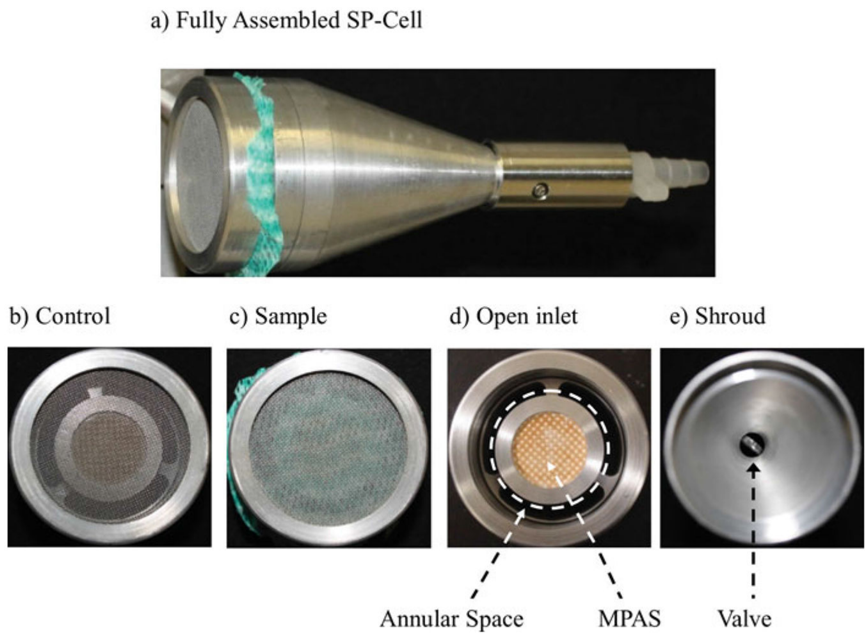

Figure 1.
SP-Cell components: a) fully assembled SP-Cell; b) control (without fabric); c) sample (with fabric); d) inlet without screen showing annular space for air flow and MPAS; and e) butterfly flow control valve housed in shroud.

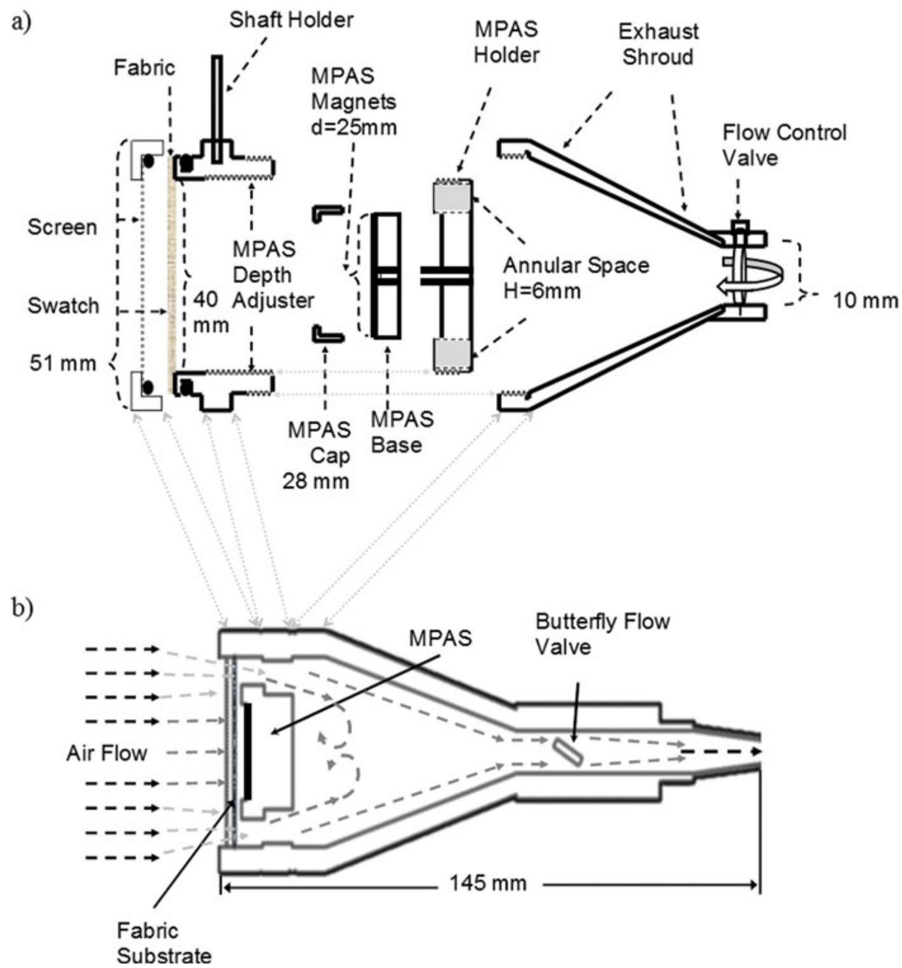

Figure 2.

MPAS housed in shrouded cell: a) components; b) constructed with line-drawn air-flow lines.

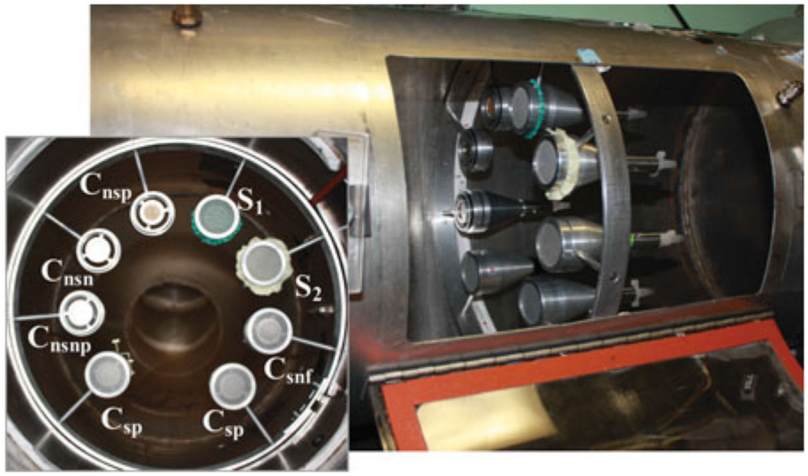

Figure 3.

SP-Cells arranged on a support ring in the RAWT. A variety of setup configurations are presented for demonstration purposes, including SP-Cell: 1) with swatch samples (S_1, S_2); and 2) controls (C) [with screen, but no filter (C_{snf}), with screen and collected particles (C_{sp}), without Screen with collected particles (C_{nsp}) and without screen, without collected particles (C_{nsnp})].

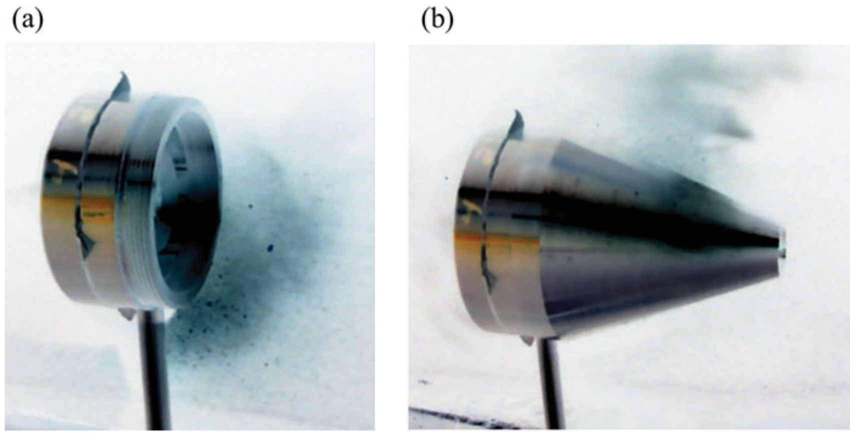

Figure 4.
Transport pattern of air tracked by smoke at 0.5 m/s, without and with shroud.

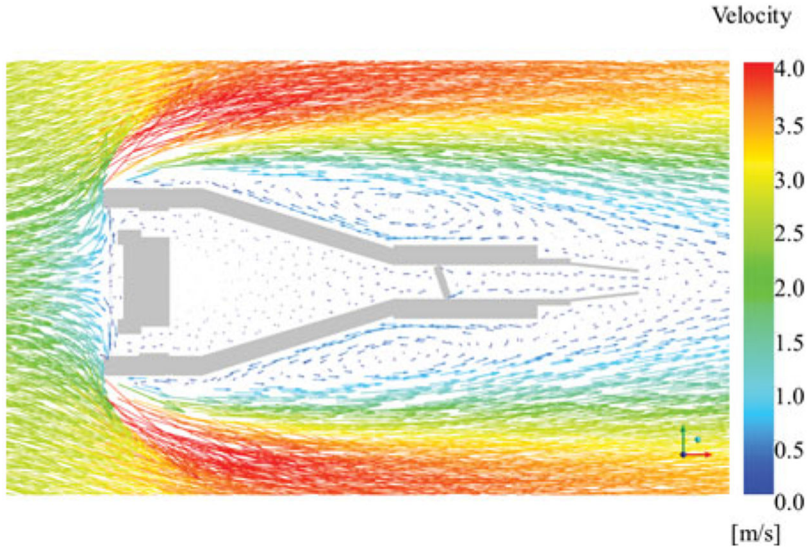

Figure 5.
Velocity vector field at a typical ambient wind speed of 2.5 m/s.

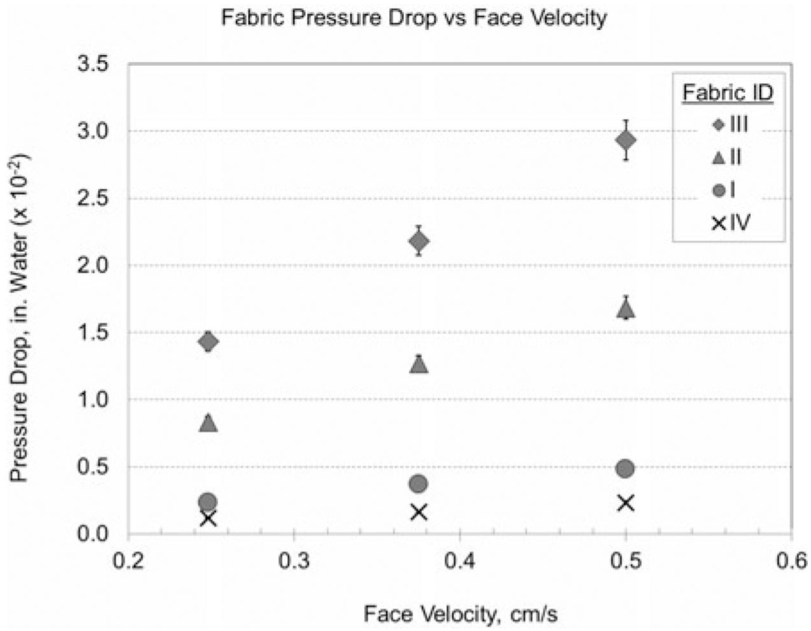

Figure 6.

Pressure drop across fabric as a function of face velocity.

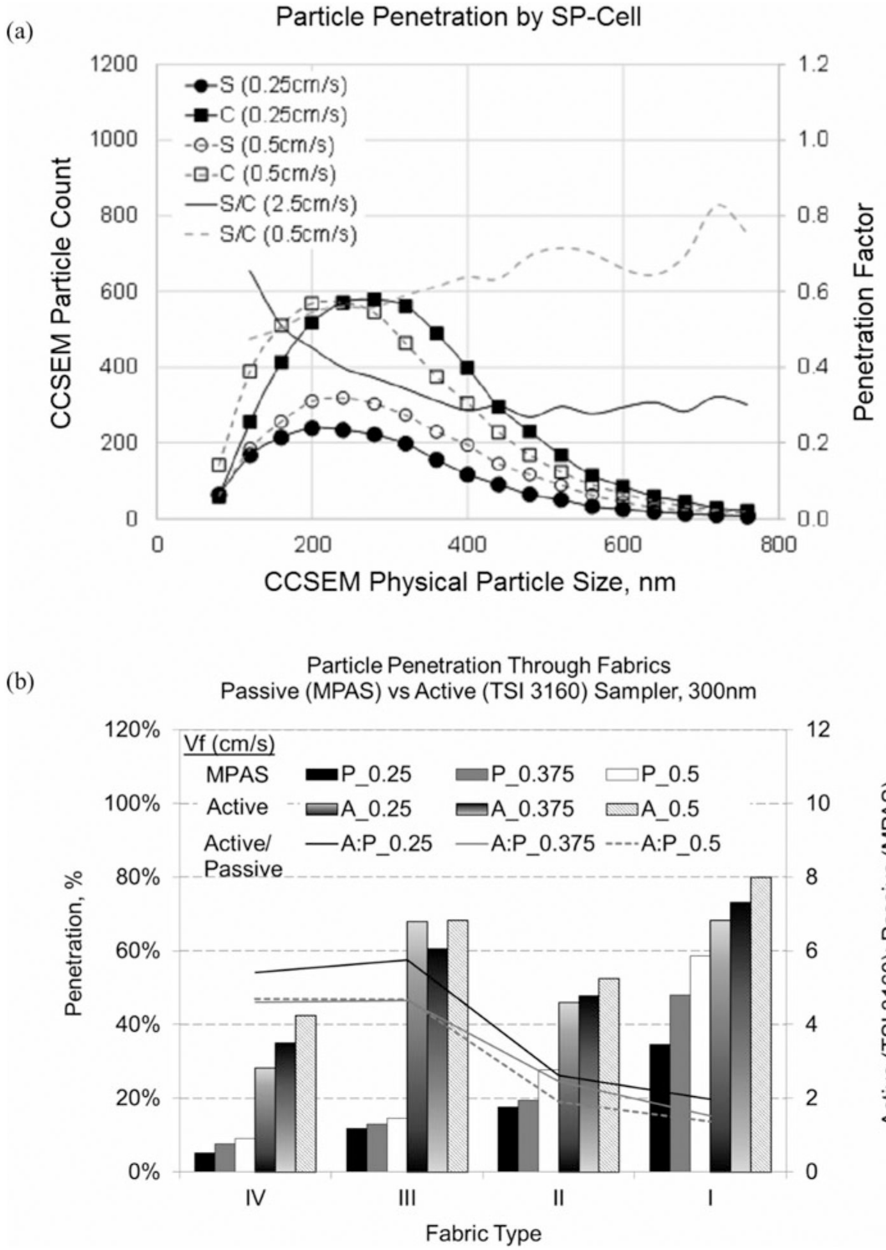

Figure 7.

Particle Penetration: (a) fabric I, at two face velocities, by SP-Cell with Sample (S) and Control (C) and Fractional Penetration (S/C); and (b) comparing passive to active sampler measurements of four garment models.

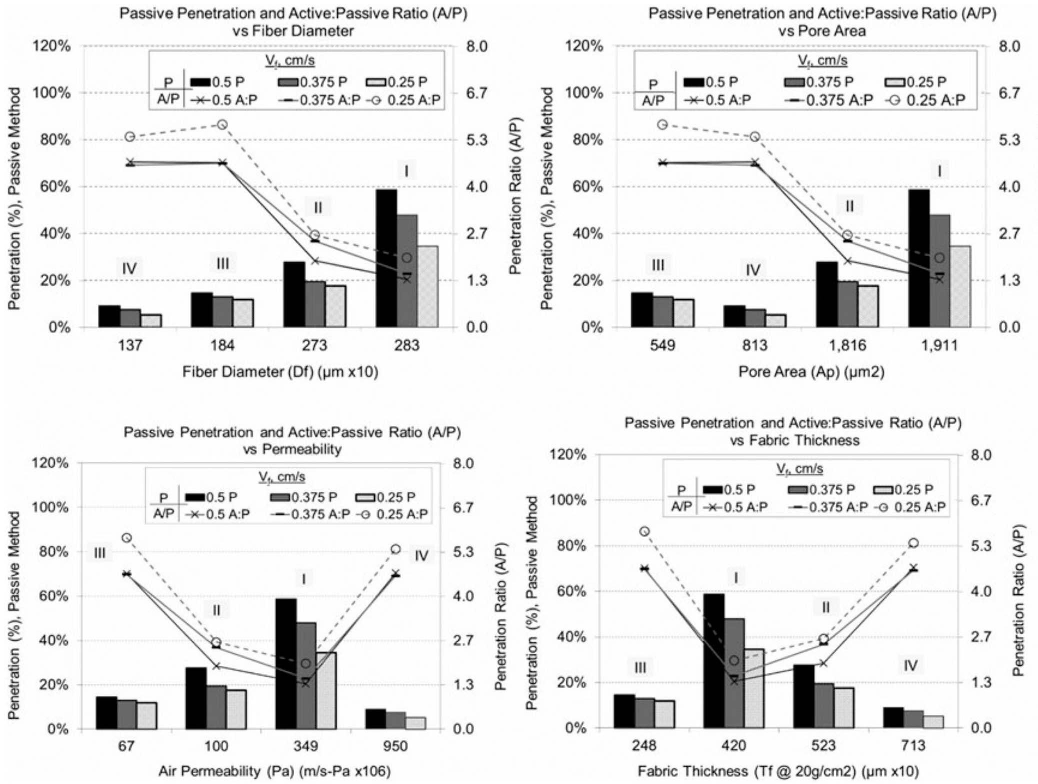

Figure 8.

Penetration by the passive method with comparison against four physical measures of fabric (fabric diameter, pore area, air permeability, and fabric thickness) for all four tested garments (I, II, III, and IV).

Table 1.

List of the tested nonwoven fabrics.

ID	Material	Application	Structural Feature
I	Cellulose	Solvent Cleaning Cloth	Resembling patterned wet-laid structure
II	Cellulose	Cleaning Cloth	two adhesive bonded layers reinforced by yarns between the layers
III	Cellulose	Machinery Wiping Cloth	4-layer structure, resembling wet-laid structure, reinforced with yarns along the length and width directions between the middle two layers
IV	Meta-aramid	Fire fighter ensemble insulation	Most likely needle-punched fabric

Table 2.

Physical properties of the nonwoven fabrics.

ID	Fiber Diameter (μm)	Thickness (μm)	Porosity	Air Permeability (m/sec-Pa)	Pore Volume × 10^{-3} (m^3/Kg)	Pore Radius (μm)
I	28.29 (34.0%)	420 (2.7%)	0.8589	0.00349 (12.8%)	3.95 (0.44%)	24.67
II	27.30 (34.9%)	523 (3.9%)	0.8612	0.00100 (8.0%)	4.03 (0.54%)	24.05
III	18.37 (38.1%)	222 (3.5%)	0.8056	0.00067 (14.7%)	2.69 (0.93%)	13.22
IV	13.65 (11.7%)	713 (2.2%)	0.9174	0.00950 (4.4%)	8.11 (0.2%)	16.09

Notes: The numbers in parentheses represent the values of the coefficient of variation for the properties. The CV% values of porosity, pore volume, and pore size were exactly the same and very small. This is because these parameters are calculated from models that involve only the ratio of fabric thickness to fabric weight per unit area and constants. Variability found in the value of fabric thickness is largely due to the variability that exists in fabric weight. Accordingly, when the ratio of the thickness to the weight is taken, the variability greatly diminishes.